Dynamic optimization methodology based on subgrid-scale dissipation for large eddy simulation

Changping Yu, Zuoli Xiao, and Xinliang Li

Citation: Physics of Fluids **28**, 015113 (2016); doi: 10.1063/1.4940044
View online: http://dx.doi.org/10.1063/1.4940044
View Table of Contents: http://scitation.aip.org/content/aip/journal/pof2/28/1?ver=pdfcov
Published by the AIP Publishing

Dynamic optimization methodology based on subgrid-scale dissipation for large eddy simulation

Changping Yu,[1] Zuoli Xiao,[2] and Xinliang Li[1,a)]
[1]*LHD, Institute of Mechanics, Chinese Academy of Sciences, Beijing 100190, People's Republic of China*
[2]*State Key Laboratory for Turbulence and Complex Systems, College of Engineering, Peking University, Beijing 100871, People's Republic of China*

(Received 16 September 2015; accepted 5 January 2016; published online 27 January 2016)

A dynamic procedure based on subgrid-scale dissipation is proposed for large eddy simulation of turbulent flows. In the new method, the model coefficients are determined by minimizing the square error of the resolved dissipation rate based on the Germano identity. A dynamic two-term mixed model is tested and evaluated both *a priori* and *a posteriori* in simulations of homogeneous and isotropic turbulence. The new dynamic procedure proves to be more effective to optimize the model coefficients as compared with traditional method. The corresponding dynamic mixed model can predict the physical quantities more accurately than traditional dynamic mixed model. © *2016 AIP Publishing LLC.* [http://dx.doi.org/10.1063/1.4940044]

As an important numerical simulation method of turbulent flows, large eddy simulation (LES) has been widely applied to scientific research[1–3] and engineering prediction of turbulence.[4–6] Several different subgrid-scale (SGS) models have been proposed, such as Smagorinsky model (SM),[7] similarity model,[8] gradient model (GM),[9] mixed model,[10,11] and eddy-viscosity model based on helicity.[12] At the same time, some methods have also been developed to optimize the SGS models. The widely used approach is the traditional dynamic method which is based on the Germano identity[13]

$$L_{ij} = T_{ij} - \overline{\tau}_{ij}, \tag{1}$$

where $L_{ij} = \overline{\widetilde{u}_i\widetilde{u}_j} - \overline{\widetilde{u}}_i\overline{\widetilde{u}}_j$ is resolved stress, τ_{ij} is the SGS stress, T_{ij} is the subtest-scale (STS) stress. The *tilde* and the *overbar* denote spatial filtering at the grid scale Δ and a test scale $\beta\Delta$, respectively. It should be mentioned that the test-filtered quantities are at scale $\alpha\Delta$ $(1 < \alpha \leqslant 2)$. For spectral sharp cut-off filter, β is equal to α. For Gaussian filter, as used in this letter, however, β is equal to $\sqrt{\alpha^2 - 1}$. Substituting τ_{ij}^{mod} and T_{ij}^{mod} for τ_{ij} and T_{ij} in Eq. (1), one gets

$$L_{ij}^{mod} = T_{ij}^{mod} - \overline{\tau}_{ij}^{mod}. \tag{2}$$

For Smagorinsky model, we have

$$\tau_{ij}^{mod} - \frac{1}{3}\delta_{ij}\tau_{kk}^{mod} = -2C_s\Delta^2|\widetilde{S}|\widetilde{S}_{ij}, \tag{3}$$

$$T_{ij}^{mod} - \frac{1}{3}\delta_{ij}T_{kk}^{mod} = -2C_s(\alpha\Delta)^2|\overline{\widetilde{S}}|\overline{\widetilde{S}}_{ij}, \tag{4}$$

where $\widetilde{S}_{ij} = \left(\partial_j\widetilde{u}_i + \partial_i\widetilde{u}_j\right)/2$ is the resolved strain rate tensor at the grid scale, $|\widetilde{S}| = (2\widetilde{S}_{ij}\widetilde{S}_{ij})^{1/2}$, and C_s is the model coefficient. The Germano identity denoted by Smagorinsky model can be expressed as

$$L_{ij}^{mod} = \frac{1}{3}\delta_{ij}L_{kk}^{mod} - C_s(2\alpha^2\Delta^2|\overline{\widetilde{S}}|\overline{\widetilde{S}}_{ij} - 2\Delta^2\overline{|\widetilde{S}|\widetilde{S}_{ij}}). \tag{5}$$

Germano *et al.* put forward the original dynamic method,[14] which contracts Eq. (5) with $\widetilde{S}_{ij}$ to obtain the model coefficient. This method has no obvious physical meaning,[15] and cannot be

a)Author to whom correspondence should be addressed. Electronic mail: lixl@imech.ac.cn

applied to mixed model. The dynamic procedure has been subsequently modified and refined by Lilly, Piomelli, and Meneveau *et al.*[15–17] and becomes the most commonly used method for SGS model optimization. In this method, the least-squares method is used to minimize the ensemble average (denoted by $\langle\cdot\rangle$, which can be regarded as the spatial average over statistically homogeneous regions) of square error of the resolved stress,

$$E = \langle (L_{ij} - L_{ij}^{mod})^2 \rangle, \tag{6}$$

to obtain the model coefficient. Recently, Shi *et al*. suggest the dynamic mixed model (DMM) under the constraint on energy fluxes through two different scales.[18] The constraint of helicity flux and the joint-constraint of energy and helicity fluxes are proposed by Yu *et al*. to constrain the dynamic mixed SGS model for LES of helical turbulence.[19,20] Meneveau redefines the Germano identity with a generalized style which can improve the simulation result in dynamic model for LES of turbulence.[21]

A proper dynamic method for optimizing the SGS model should have explicit physical meaning in order to model the SGS effect on the large-scale motions. In this letter, we suggest a new dynamic procedure based on the SGS energy dissipation rate for LES of turbulent flows. We select the mixed model, which is composed of the SM term and the GM term, to discuss the features of the present dynamic optimization method.

For LES of incompressible turbulent flow, we need solve the filtered Navier-Stokes equations,

$$\partial_t \widetilde{u}_i + \partial_j(\widetilde{u}_i \widetilde{u}_j) = -\frac{1}{\rho}\partial_i \widetilde{p} + \nu \partial_j \partial_j \widetilde{u}_i + \widetilde{f}_i - \partial_j \tau_{ij}, \tag{7}$$

where $\tilde{f}_i$ is the filtered driving force, and $\tau_{ij} = \widetilde{u_i u_j} - \widetilde{u}_i \widetilde{u}_j$ is the SGS stress tensor generated by motions of small scales less than Δ.

From Eq. (7), we can obtain the conservation equation of the resolved kinetic energy $E_\Delta = \widetilde{\boldsymbol{u}} \cdot \widetilde{\boldsymbol{u}}/2$ as follows:

$$\partial_t E_\Delta + \partial_j \left(\widetilde{u}_j E_\Delta\right) = \partial_j \widetilde{J}_j - 2\nu \widetilde{S}_{ij}\widetilde{S}_{ij} + 2\widetilde{f}_i \widetilde{u}_i - \Pi_\Delta, \tag{8}$$

where $\widetilde{J}_j = \widetilde{u}_i(2\nu\widetilde{S}_{ij} - \frac{\widetilde{p}}{\rho}\delta_{ij} - \tau_{ij})$ is the spatial transport term of the large-scale kinetic energy and $\Pi_\Delta = -\tau_{ij}\widetilde{S}_{ij}$ is the local SGS dissipation (or the energy flux across scale Δ).

In LES, τ_{ij} and Π_Δ are two important quantities and need to be determined by SGS model. For different SGS models, the pointwise correlation coefficients can evaluate the relevance between the modeled SGS stress and the real SGS stress or the relevance between the modeled energy flux and the real energy flux. The expression of the correlation coefficient ρ is

$$\rho = \frac{\langle (M - \langle M \rangle)(R - \langle R \rangle) \rangle}{(\langle (M - \langle M \rangle)^2 \rangle \langle (R - \langle R \rangle)^2 \rangle)^{1/2}}, \tag{9}$$

where M denotes the component of the SGS stress model or the modeled energy flux, and R denotes the component of the real SGS stress or the real energy flux. A two-term mixed SGS and STS models are selected here as

$$\tau_{ij}^{mod} = C_{sm}\Delta^2 |\widetilde{S}| \widetilde{S}_{ij} + C_{gm}\Delta^2 \partial_k \widetilde{u}_i \partial_k \widetilde{u}_j, \tag{10}$$

$$T_{ij}^{mod} = C_{sm}(\alpha\Delta)^2 |\overline{\widetilde{S}}| \overline{\widetilde{S}}_{ij} + C_{gm}(\alpha\Delta)^2 \partial_k \overline{\widetilde{u}}_i \partial_k \overline{\widetilde{u}}_j, \tag{11}$$

where C_{sm} and C_{gm} are the model coefficients of the Smagorinsky model term and the gradient model term, respectively. The correlation coefficients relevant to the Smagorinsky model term and the gradient model term are first evaluated *a priori* using the data from direct numerical simulations (DNS) of three dimensional incompressible homogeneous isotropic turbulence. The Navier-Stokes equations are solved numerically by using a pseudospectral code in a cubic box with periodic boundary conditions. A Gaussian random field is used as the initial condition, which has an energy spectrum in the form $E_0(k) = Ak^2 U_0^2 k_0^{-5} e^{-2k^2/k_0^2}$, where $k_0 = 4.5786$, $U_0 = 0.715$, and A is selected such that the initial kinetic energy is equal to $3U_0^2/2$. The whole system is maintained by a constant energy input rate $\epsilon = 0.1$ in the first two wave-number shells. The numerical resolution is 512^3 and the kinematic viscosity $\nu = 6 \times 10^{-4}$. A Gaussian filter function is used for data analysis.

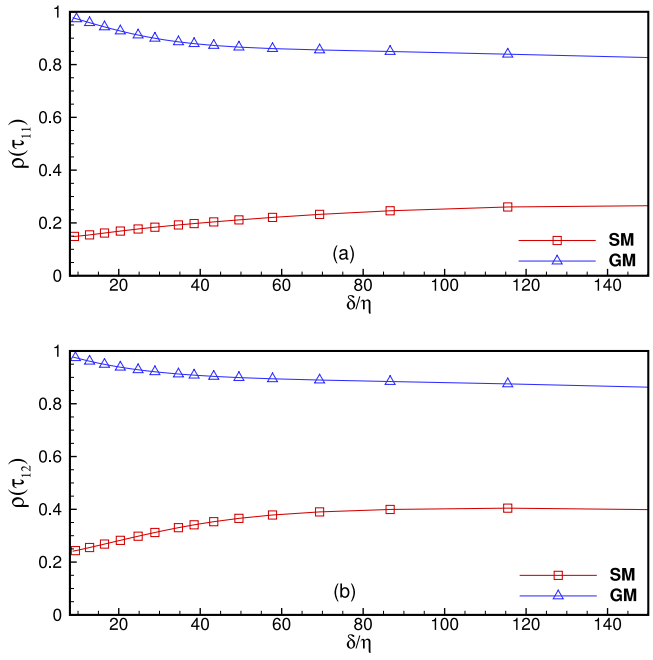

FIG. 1. Correlation coefficients between components of the real SGS stress and component of SM and GM with respect to the normalized filter width obtained *a priori* using DNS data. (a) $\rho(\tau_{11})$ and (b) $\rho(\tau_{12})$. η is the Kolmogorov length scale.

Shown in Figs. 1(a) and 1(b) are the behaviors of $\rho(\tau_{11})$ and $\rho(\tau_{12})$ as a function of the normalized filter width δ/η, where δ is the filter width varying from small scale to large scale and η is the Kolmogorov length scale. We can see clearly that the correlation coefficients $\rho(\tau_{11})$ and $\rho(\tau_{12})$ of GM decrease monotonically with the filter width and are greater than 0.85 within the whole range of δ. However, $\rho(\tau_{11})$ and $\rho(\tau_{12})$ of SM show different behaviors from those of GM and increase monotonically with the filter width. Neither $\rho(\tau_{11})$ nor $\rho(\tau_{12})$ for SM is greater than 0.4. Displayed in Fig. 2 are the correlation coefficients of SGS energy dissipation rate $\rho(\Pi_\delta)$ versus the normalized filter width δ/η from *a priori* test of GM and SM. It is seen that $\rho(\Pi_\delta)$ of GM and that of SM have little difference with each other, and meanwhile, both of them have high values on almost every filter width, greater than 0.8.

The least-squares method will overestimate the coefficient of undetermined quantity which has high correlation with the known quantity, and conversely will underestimate it. Thus, the traditional dynamic method based on resolved stress will overestimate GM term and underestimate SM term in the mixed model. Here, a new dynamic method based on SGS dissipation is proposed to solve this problem.

Using Germano identity (1), the expression of the SGS energy dissipation rate at the subtest-scale $\alpha\Delta$ can be written as follows:

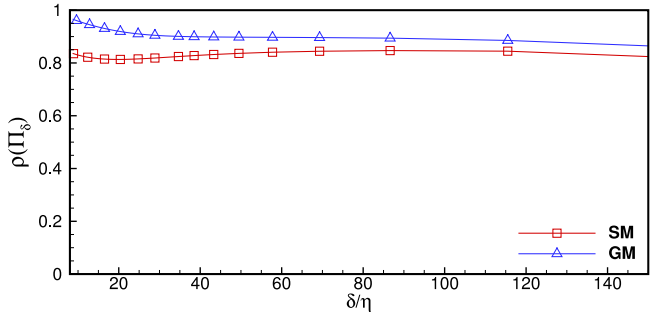

FIG. 2. Correlation coefficients $\rho(\Pi_\delta)$ between the real energy flux and the modeled energy flux caused by DM and GM with respect to the normalized filter width obtained *a priori* using DNS data.

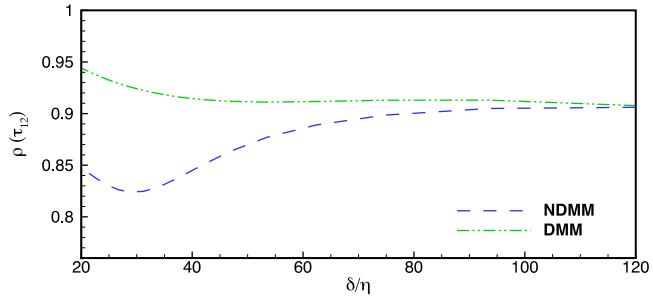

FIG. 3. Correlation coefficients $\rho(\tau_{12})$ between component of the real SGS stress τ_{12} and the modeled τ_{12} from NDMM (dashed line) and DMM (dashed-double dotted line) with respect to the normalized filter width obtained *a priori* using DNS data.

$$\Pi_{\alpha\Delta} = -L_{ij}\overline{\overline{S}}_{ij} - \overline{\tau}_{ij}\overline{\overline{S}}_{ij}, \tag{12}$$

where $\Pi_{\alpha\Delta} = -T_{ij}\overline{\overline{S}}_{ij}$, and $-L_{ij}\overline{\overline{S}}_{ij}$ is the resolved energy dissipation rate. From Eq. (12), the square error of the resolved energy dissipation rate is

$$E^{mod}_{\alpha\Delta} = \langle(-L_{ij}\overline{\overline{S}}_{ij} + (T^{mod}_{ij} - \overline{\tau}^{mod}_{ij})\overline{\overline{S}}_{ij})^2\rangle. \tag{13}$$

Substituting Eqs. (10) and (11) into Eq. (13), and using the least-square approach, we can obtain the coefficients of SM and GM terms,

$$C_{sm} = \frac{\langle M_{SM}L_{ij}\overline{\overline{S}}_{ij}\rangle\langle M^2_{GM}\rangle - \langle M_{GM}L_{ij}\overline{\overline{S}}_{ij}\rangle\langle M_{SM}M_{GM}\rangle}{\langle M^2_{SM}\rangle\langle M^2_{GM}\rangle - \langle M_{SM}M_{GM}\rangle^2}, \tag{14}$$

$$C_{gm} = \frac{\langle M_{GM}L_{ij}\overline{\overline{S}}_{ij}\rangle\langle M^2_{SM}\rangle - \langle M_{SM}L_{ij}\overline{\overline{S}}_{ij}\rangle\langle M_{SM}M_{GM}\rangle}{\langle M^2_{SM}\rangle\langle M^2_{GM}\rangle - \langle M_{SM}M_{GM}\rangle^2}, \tag{15}$$

where $M_{SM} = \Delta^2(\alpha^2|\overline{\overline{S}}|\overline{\overline{S}}_{ij} - \overline{|\overline{S}|\overline{S}_{ij}}\overline{\overline{S}}_{ij})$ and $M_{GM} = \Delta^2(\alpha^2\partial_k\overline{\overline{u}}_i\partial_k\overline{\overline{u}}_j\overline{\overline{S}}_{ij} - \overline{\partial_k\widetilde{u}_i\partial_k\widetilde{u}_j}\overline{\overline{S}}_{ij})$.

First, the new dynamic method is validated *a priori* by using the DNS data mentioned above. For this purpose, the new dynamic mixed model (NDMM) is compared with the traditional DMM.

The pointwise correlation of the modeled SGS stress with the real SGS stress is an important criterion to evaluate the property of the SGS models. By *a priori* test, we can get the result that the pointwise correlation coefficients of τ_{12} from NDMM and DMM are both greater than 0.85 in inertial subrange, which is displayed in Fig. 3. We show in Fig. 4 the probability density functions

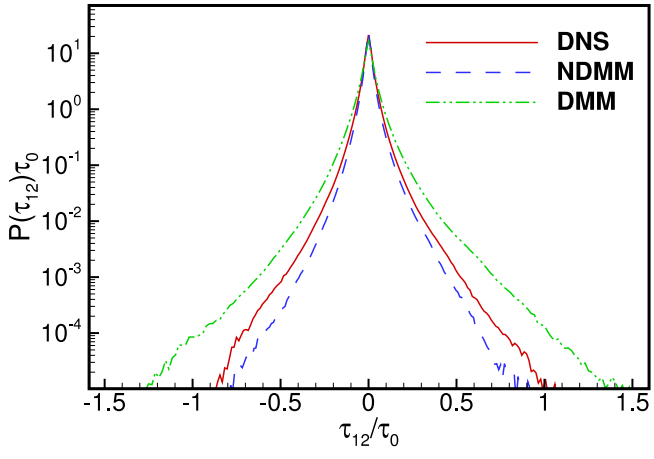

FIG. 4. The PDFs of the modeled SGS stress τ_{12} at a filter width $\Delta = 80\eta$: NDMM (dashed line), DMM (dashed-double dotted line), and DNS (the bold solid line). The horizontal axis is normalized by the characteristic stress $\tau_0 = U_0^2/2$.

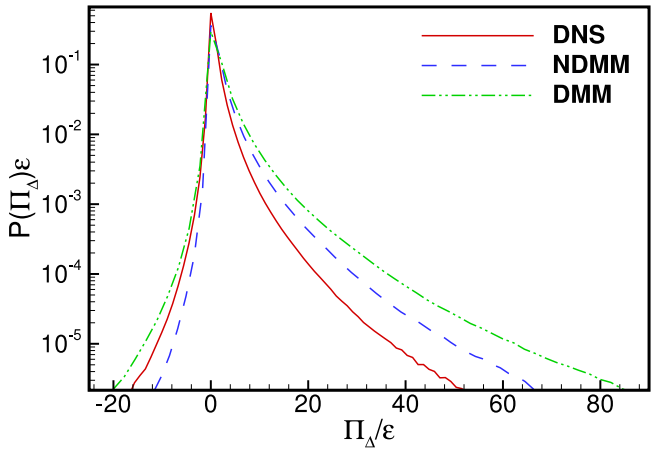

FIG. 5. The PDFs of the local energy flux Π_Δ at a filter length $\Delta = 80\eta$ calculated by use of different SGS models: NDMM (dashed line), DMM (dashed-double dotted line), and DNS (the bold solid line). The horizontal axis is normalized by the energy injection rate ε.

(PDFs) of the component of the modeled SGS stress τ_{12} and that of the real τ_{12} at a filter width $\Delta = 80\eta$. We can see that the PDF for DMM is much wider than the real SGS stress, while the PDF for NDMM is much closer to the latter. Shown in Fig. 5 are the PDFs of the modeled energy flux Π_Δ across the given filter scale $\Delta = 80\eta$. It is shown that the pdf of NDMM is closer to the DNS curve, especially for the positive branch. Both of the two models can predict the phenomena of backscatters which are important physical processes of energy transfer in turbulence.

In Fig. 6, we show the r.m.s values of τ_{12} from NDMM, DMM, and DNS. We can see that the value from DMM is greater than that from DNS, and while the result from NDMM is less than the DNS value. Fig. 7 displays the absolute value of the difference between the modelled τ_{12} and the real one versus the varying filter length. From the figure, we can see that the value from NDMM is smaller than that from DMM, which indicates that τ_{12}^{mod} from NDMM is closer to the real τ_{12}. In Fig. 8, we show the mean energy flux through δ as a function of δ/η for NDMM, DMM, and DNS. It is clear that the result predicted by NDMM is closer to DNS value than that by DMM at most of the δ.

The intermittency effects of turbulent energy cascade can be explained by the refined similarity hypothesis (RSH) introduced by Kraichnan.[22] Adopting the method of Chen *et al.*,[23] we show in Figs. 9(a) and 9(b) different order moment of the normalized energy flux $\langle(|\delta\Pi_\delta|/u'^3)^{p/3}\rangle$ (p = 1, 3, 6, and 8) as function of the normalized filter width δ/η for NDMM and DMM, respectively, and the results from DNS are also displayed for comparison. It can be seen from the figures that the energy flux structure functions predicted by NDMM are approached to the results from DNS more closely than those of DMM for every p in the inertial subrange.

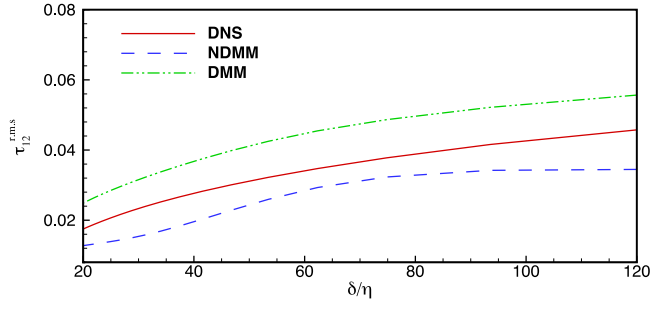

FIG. 6. The r.m.s value of τ_{12} versus the normalized filter δ/η for *a priori*: NDMM (dashed line), DMM (dashed-double dotted line), and DNS (the bold solid line).

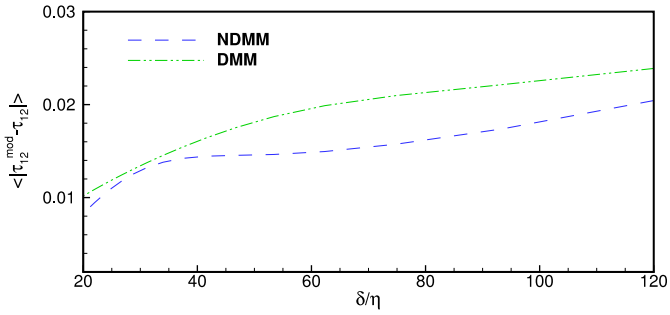

FIG. 7. The absolute value of the difference between τ_{12}^{mod} and the real τ_{12} versus the normalized filter δ/η for *a priori*: NDMM (dashed line) and DMM (dashed-double dotted line).

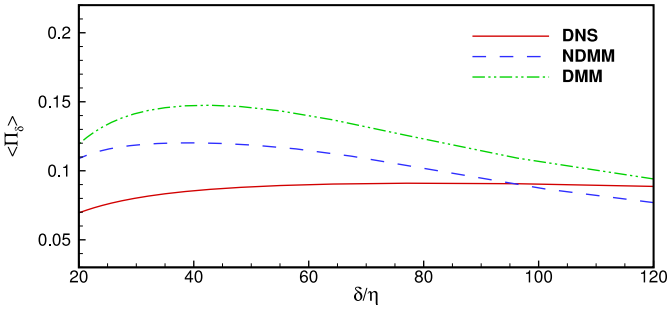

FIG. 8. The mean energy flux versus the normalized filter scale δ/η for *a priori*: NDMM (dashed line), DMM (dashed-double dotted line), and DNS (the bold solid line).

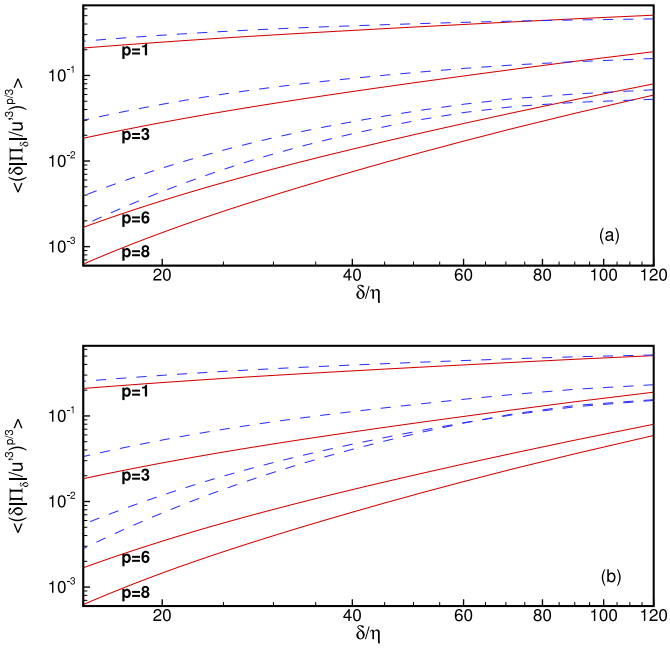

FIG. 9. Moments of the normalized energy flux of order p/3 (where $p = 1, 3, 6$, and 8) as functions of the normalized filter scale δ/η: (a) NDMM, and (b) DMM. The dashed lines: results of the models; the solid lines: results of DNS. u' is the r.m.s. velocity.

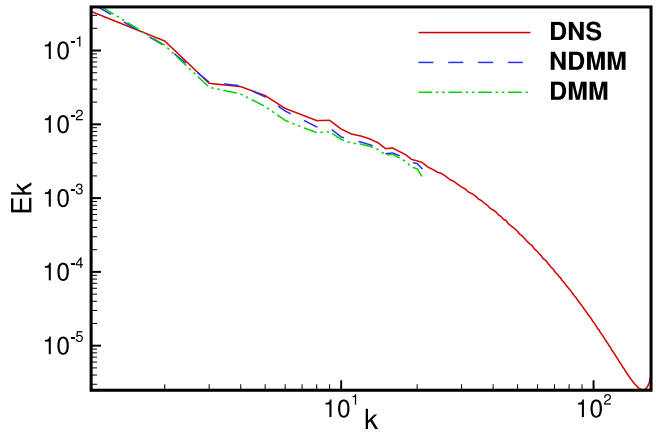

FIG. 10. Energy spectra from LESs using different SGS models: NDMM (dashed line), DMM (dashed-double dotted line), and the energy spectrum from DNS.

The new dynamic method is also tested *a posteriori* in LES of forced and freely decaying incompressible homogeneous isotropic turbulence. Filtered Navier-Stokes equations (7) were numerically solved for the forced case. The numerical algorithm and settings are the same as those for DNS mentioned above. For the decaying case, the energy input rate $\varepsilon = 0$. The grid resolution is 64^3.

Fig. 10 shows the energy spectra obtained from LESs using NDMM and DMM, and the DNS spectrum is plotted for comparison. It is noted that NDMM can predict the energy spectrum better than DMM for almost all the wavenumbers, especially in the middle-wave-number range. The model coefficients of SM model term (C_{sm}) and GM model term (C_{gm}) from different models can show the optimization effects of the two dynamic methods directly. The absolute value of C_{sm} obtained for NDMM is about 0.023, while that for DMM is about 0.017, which means that the effects of SM model term in NDMM prevail over that in DMM. The value of C_{gm} obtained for NDMM is about 0.078, and it is obviously smaller than that for DMM which is about 0.146. The value of C_{gm} for NDMM is much closer to the standard value of the GM coefficient, i.e., 1/12, while DMM overestimates C_{gm} obviously.

The new dynamic method is also tested *a posteriori* in freely decaying isotropic turbulence. A statistically steady flow field is extracted from the DNS data as the initial condition of the computation. Shown in Fig. 11 is the evolution of the mean energy $\langle E \rangle$ calculated using different models with respect to the normalized time t/τ_0 in LES of freely decaying isotropic turbulence. $\langle E \rangle$ obtained from the filtered DNS data of freely decaying flow is plotted for comparison. $\langle E \rangle$ from

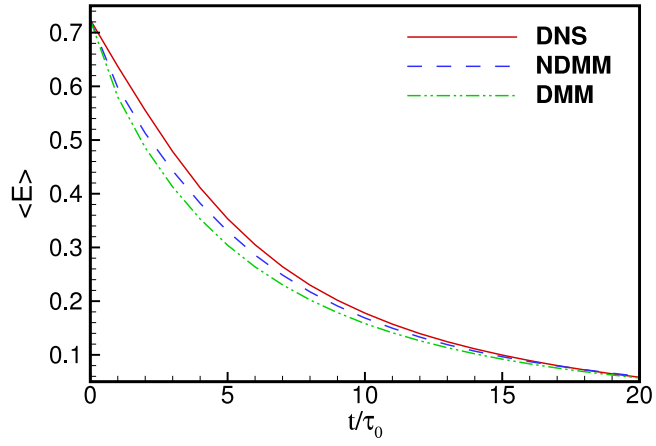

FIG. 11. The evolution of the mean energy in regard to t/τ_0 calculated *a posteriori* in freely decaying isotropic turbulence. NDMM (the dashed line), DMM (dashed-double dotted line), and the mean energy from DNS (bold solid line).

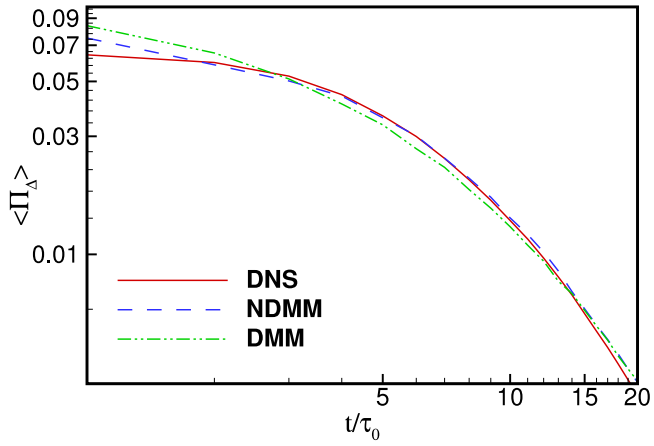

FIG. 12. The evolution of SGS energy dissipation across filter width Δ in regard to t/τ_0 calculated *a posteriori* in freely decaying turbulence. NDMM (the dashed line), DMM (dashed-double dotted line), and the real SGS dissipation from DNS (bold solid line).

NDMM is much closer to the DNS result than that from DMM in almost the whole decay process. In Fig. 12, we display the mean energy flux through a filter scale predicted by NDMM, DMM, and DNS with respect to the normalized time t/τ_0 in the freely decaying isotropic turbulence. We can see that the curve of $\langle \Pi_\Delta \rangle$ predicted by NDMM almost collapses onto the real energy flux, and obvious improvement is observed compared with the result predicted by DMM.

The new method has been also applied to optimize other SGS models in LES. For the similarity mixed model,[10] both of the tested results from the two methods are not so good, but the new method still has the obvious advantage in contrast with the traditional one. For the Smagorinsky model, the new method has negligible advantage over the traditional one. And after analyzing the expressions of model coefficients predicted by the two dynamic methods, we know that it is the special modelling form of Smagorinsky model that causes the similar results by the different methods.

In summary, a new dynamic method based on energy flux at the subtest-scale is proposed for SGS modeling in large eddy simulation of turbulent flows, which is physically different from the traditional dynamic procedure based on resolved stress. Compared with traditional dynamic method, the new method of minimizing the SGS dissipation error can keep the dissipation to approach the real dissipation of the flow field, which is the assurance of obtaining the better results. Both *a priori* and *a posteriori* tests have been conducted to assess the performance of the new dynamic mixed model in simulation of homogeneous and isotropic turbulence. Compared with the traditional dynamic mixed model, the new dynamic mixed model proves to provide better predictions in energy spectrum, energy flux, intermittency of energy cascade, etc. Therefore, it is suggested that the present dynamic method shall serve as a useful option for optimization of the coefficients of SGS models. The new dynamic optimization method can be used in channel flow and other inhomogeneous turbulence, and it will be shown in a future paper.

We wish to thank Dexun Fu and Yanwen Ma for fruitful discussions on this work. This work was supported by the NSFC Projects (Nos. 11472278, 91441103, 11372007, and 11372330), the 863 Program (No. 2012AA01A304), and the CAS Program (Nos. KJCX2-EW-J01 and XXH12503-02-02-04).

[1] Y. Ponty and H. Politano, "Simulation of induction at low magnetic Prandtl number," Phys. Rev. Lett. **92**, 144503 (2004).
[2] W. Anderson and M. Chamecki, "Numerical study of turbulent flow over complex aeolian dune fields: The White Sands National Monument," Phys. Rev. E **89**, 013005 (2014).
[3] I. Bermejo-Moreno, L. Campo, J. Larsson, J. Bodart, D. Helmer, and J. K. Eaton, "Confinement effects in shock wave/turbulent boundary layer interactions through wall-modelled large-eddy simulations," J. Fluid Mech. **758**, 5 (2014).
[4] A. Dauptain, L. Y. M. Gicque, and S. Moreau, "Large eddy simulation of supersonic impinging jets," AIAA J. **50**, 1560 (2012).
[5] S. Acharya and D. H. Leedom, "Large eddy simulations of discrete hole film cooling with plenum inflow orientation effects," J. Heat Transfer **135**, 011010 (2013).

[6] F. Xiao, M. Dianat, and J. J. McGuirk, "Large eddy simulation of liquid-jet primary breakup in air crossflow," AIAA J. **51**, 2878 (2013).
[7] J. S. Smagorinsky, "General circulation experiments with the primitive equations: I. The basic experiment," Mon. Weather Rev. **91**, 99 (1963).
[8] J. Bardina, J. H. Ferziger, and W. C. Reynolds, "Improved subgrid scale models for large eddy simulation," AIAA Paper No. 80-1357 (1980).
[9] R. A. Clark, "Evaluation of subgrid-scale models using an accurately simulated turbulent flow," J. Fluid Mech. **91**, 1 (1996).
[10] Y. Zang, R. L. Street, and J. R. Koseff, "A dynamic mixed subgrid-scale model and its application to turbulent recirculating flows," Phys. Fluids A **5**, 3186 (1993).
[11] B. Vreman, B. Geurts, and H. Kuerten, "Large-eddy simulation of the temporal mixing layer using the Clark model," Theor. Comput. Fluid Dyn. **8**, 309 (1996).
[12] C. Yu, R. Hong, Z. Xiao, and S. Chen, "Subgrid-scale eddy viscosity model for helical turbulence," Phys. Fluids **25**, 095101 (2013).
[13] M. Germano, "Turbulence: The filtering approach," J. Fluid Mech. **238**, 325 (1992).
[14] M. Germano, U. Piomelli, P. Moin, and W. H. Cabot, "A dynamic subgrid-scale eddy viscosity model," Phys. Fluids A **3**, 1760 (1991).
[15] D. K. Lilly, "A proposed modification of the Germano subgrid-scale closure method," Phys. Fluids A **4**, 3 (1992).
[16] U. Piomelli, "High Reynolds number calculations using the dynamic subgrid-scale stress model," Phys. Fluids A **5**, 1484 (1993).
[17] C. Meneveau, T. S. Lund, and W. H. Cabot, "A Lagrangian dynamic subgrid-scale model turbulence," J. Fluid Mech. **319**, 353 (1996).
[18] Y. Shi, Z. Xiao, and S. Chen, "Constrained subgrid-scale stress model for large eddy simulation," Phys. Fluids **20**, 011701 (2008).
[19] C. Yu and Z. Xiao, "Refined subgrid-scale model for large-eddy simulation of helical turbulence," Phys. Rev. E **87**, 013006 (2013).
[20] C. Yu, Z. Xiao, Y. Shi, and S. Chen, "Joint-constraint model for large-eddy simulation of helical turbulence," Phys. Rev. E **89**, 043021 (2014).
[21] C. Meneveau, "Germano identity-based subgrid-scale modeling: A brief survey of variations on a fertile theme," Phys. Fluids **24**, 12301 (2012).
[22] R. H. Kraichnan, "On Kolmogorovs inertial-range theories," J. Fluid Mech. **62**, 305 (1974).
[23] Q. Chen, S. Chen, G. L. Eyink, and D. D. Holm, "Intermittency in the joint cascade of energy and helicity," Phys. Rev. Lett. **90**, 214503 (2003).